Density-dependent energy relaxation of hot electrons in InN epilayers

M. D. Yang, Y. W. Liu, J. L. Shen, C. W. Chen, G. C. Chi, T. Y. Lin, W. C. Chou, M. H. Lo, H. C. Kuo, and T. C. Lu

Citation: Journal of Applied Physics **105**, 013526 (2009); doi: 10.1063/1.3056383
View online: http://dx.doi.org/10.1063/1.3056383
View Table of Contents: http://scitation.aip.org/content/aip/journal/jap/105/1?ver=pdfcov
Published by the AIP Publishing

Density-dependent energy relaxation of hot electrons in InN epilayers

M. D. Yang,[1] Y. W. Liu,[1] J. L. Shen,[1,a)] C. W. Chen,[2] G. C. Chi,[2] T. Y. Lin,[3] W. C. Chou,[4] M. H. Lo,[5] H. C. Kuo,[5] and T. C. Lu[5]
[1]*Department of Physics, Chung Yuan Christian University, Chung-Li, Tao Yuan 32023, Taiwan*
[2]*Department of Physics, National Central University, Chung-Li 32001, Taiwan*
[3]*Institute of Optoelectronic Sciences, National Taiwan Ocean University, Keelung, 20224, Taiwan*
[4]*Department of Electrophysics, National Chiao-Tung University, Hsin-Chu, 30010, Taiwan*
[5]*Department of Photonics and Institute of Electro-Optical Engineering, National Chiao Tung University, Hsinchu, 30010, Taiwan*

(Received 23 September 2008; accepted 17 November 2008; published online 9 January 2009)

This work investigates the dependence of the hot-electron energy relaxation in InN epilayers on electron density. From the high-energy tail of photoluminescence, the electron temperature of the hot electrons was determined. Acoustic phonons have an important role in the energy relaxation of the hot electrons. The density-dependent electron energy loss rate in InN can be explained by a combination of longitudinal optical and acoustic phonon emissions. A slowing of energy loss rate at high electron densities was observed and attributed to piezoelectric coupling to acoustic phonons.
 [DOI: 10.1063/1.3056383]

I. INTRODUCTION

Group-III nitride semiconductors have recently attracted much attention because of their applications in the ultraviolet to near infrared regions by proper alloying. Among the group-III nitride semiconductors, InN has attracted considerable attention due to its unusual physical properties and potential applications in optoelectronic devices, such as light-emitting diodes, lasers, high-speed electronics, and high-efficiency solar cells.[1–3] Studies of electron energy relaxation have produced information about the electron-lattice scattering and electron-electron scattering because the electron relaxation is associated with inelastic collisions with the phonons and electrons. An understanding of electron energy relaxation in semiconductors is thus of fundamental interest in the physics of semiconductors and is important in the design and evaluation of devices.[4–6] When excess energy is supplied to an electron by optical excitation, the photogenerated electron becomes hot. The hot electrons then relax toward a less energetic state via two competing processes—scattering with other electrons and emission of phonons.[7] The first process increases the temperature of electrons, which are thermalized among themselves due to electron-electron scattering. The thermalized electrons then transfer energy to the lattice via phonon emission. Under steady-state excitation conditions, the electron temperature can thus be determined by the interaction between the power supplied to the electrons and the power lost from the electrons to the lattice via phonon emission.

In recent years, many studies have been performed to investigate the energy relaxation of hot carriers and/or phonon lifetimes in InN. For example, Chen *et al.*[8] studied hot-electron relaxation in InN at room temperature by transient transmission, observing fast initial hot carrier cooling, followed by a slow recombination process with characteristic decay times of 300–400 ps. Zanato *et al.*[9] determined the hot-electron cooling rate via longitudinal optical (LO) phonons in InN by making high-speed *I-V* measurements. They found an effective electron-LO phonon lifetime of 200 fs and used the hot-phonon effect to explain the reduction in the rate of energy relaxation. The authors of the present work have also investigated the energy relaxation of electrons in InN epilayers by excitation- and electric field-dependent photoluminescence (PL), obtaining similar results to those of Zanato *et al.*[9] All of the cited studies suggest that LO phonon emission is the dominant energy relaxation process in InN.[8–10] However, few studies of the properties of acoustic phonons in InN are available. Tsen *et al.*[11] measured the lifetimes of the A_1(LO) and E_1(LO) phonons in InN by time-resolved Raman scattering. They demonstrated that both LO phonons decay primarily into a transverse-optical phonon with a large wave vector and an acoustic phonon with a large wave vector. However, acoustic phonon emission in the energy relaxation of hot carriers has not yet been discussed. The inelastic collisions that cause the hot electrons to lose energy may include the acoustic phonon emission, particularly at low electron temperatures. This work investigates the dependence on the electron density of electron relaxation in InN epilayers using PL. The high-energy tails of PL were characterized by effective electron temperature, which increases with excitation intensity. The energy relaxation of the hot electrons in InN can be explained by a combination of the acoustic and LO phonon emissions.

II. EXPERIMENT

InN epilayers were grown on sapphire substrates by metalorganic vapor phase epitaxy. First, a low-temperature 20-nm-thick GaN nucleation layer was deposited at 500 °C; then, a 2-μm-thick GaN layer was grown at 1000 °C. An InN layer with a thickness of 150 nm was grown on the GaN buffer layer. The details of the growth method are described elsewhere.[12] The samples were further treated by rapid ther-

a)Author to whom correspondence should be addressed. Electronic mail: jlshen@cycu.edu.tw.

TABLE I. Properties of investigated samples and parameters used for calculations of pump power per electron P_e: electron concentration n, electron mobility μ, absorption length d, the part of the photon excess energy obtained by an electron W, and ratio of LO phonon emission to the acoustic phonon emission χ.

Sample (No.)	n (cm^{-3})	μ ($cm^2/V\,s$)	d (10^{-6} cm)	W (eV)	χ (%)
A	2.4×10^{18}	978	5.20	0.467	24
B	3.3×10^{18}	948	5.25	0.584	34
C	9.0×10^{18}	916	5.30	0.895	64
D	1.4×10^{19}	758	5.58	1.040	82
E	1.6×10^{19}	540	5.70	1.123	90

mal annealing (RTA) in an environment of O_2. RTA has been proven to be an effective technique for eliminating nonradiative defects in InN and improve sample quality.[12] The annealing reduces carrier concentration and causes a redshift and a line-width narrowing of the PL band, which have been explained by a decrease in the density of defects or impurities.[12] The RTA of samples D, C, B, and A was performed with an annealing time of 30 s and a ramp rate of 30 °C/s at temperatures of 200, 300, 400 and 500 °C, respectively. (Sample E was untreated.) The electron concentrations of InN samples were obtained from the Hall-effect measurements at room temperature, and the results are shown in Table I. The PL measurements were obtained using a focused Ar ion laser operated at a wavelength of 514.5 nm as the excitation source. The sample was mounted on a closed-cycle helium cryostat at temperature of $T=15$ K. The collected luminescence was dispersed by a 0.75 m spectrometer and detected using an extended InGaAs detector.

III. RESULTS AND DISCUSSION

Figure 1 shows the high-energy tails of PL of five InN samples with different free electron densities for various excitation densities. The energy of the PL increases monotonically with the electron concentration. The blueshift in the PL peak is caused by the Burstein–Moss effect that originates from the shift in the Fermi level above the bottom of the conduction band as the electron concentration increases. The PL peak energy E_{PL} can be estimated from the Fermi energy E_F and $E_g(n)$,[13]

$$E_{PL} = E_F + E_g(n), \tag{1}$$

where n is the electron concentration and $E_g(n)$ is the carrier-concentration-dependent band gap, which approaches the band gap $E_g(n)\rightarrow E_g$ at vanishing concentration. When the nonparabolicity effect is considered, the dependence of the PL peak energy E_{PL} on concentration can be expressed as[12]

$$E_{PL} = 3.58\left(\frac{m_0}{m^*}\right)\left(\frac{n}{10^{18}}\right)^{2/3} - 1.2\times10^{-27}n^{4/3} + E_g(n), \tag{2}$$

where m_0 is the free electron mass and m^* is the effective mass of an electron. A plot of PL peak energy versus carrier concentration enables the PL spectrum to be used to estimate free carrier concentration in degenerate InN.[12]

In hot-electron PL, photoexcitation creates energetic electrons in the conduction band, which relax toward a less energetic state by transferring energy to the lattice and other electrons. If the electron-electron collision rate is larger than the phonon emission rate, then the nonequilibrium electron population in the electron gas relaxes toward a Maxwell distribution and can be characterized by an electron temperature (T_e), which is higher than the lattice temperature (T_l).[7] In Fig. 1, each tail exhibits an exponential dependence on the phonon energy, indicating that the electrons in InN are thermalized after photoexcitation, enabling a well defined T_e to be extracted. Figure 2 plots the inverse T_e versus the excita-

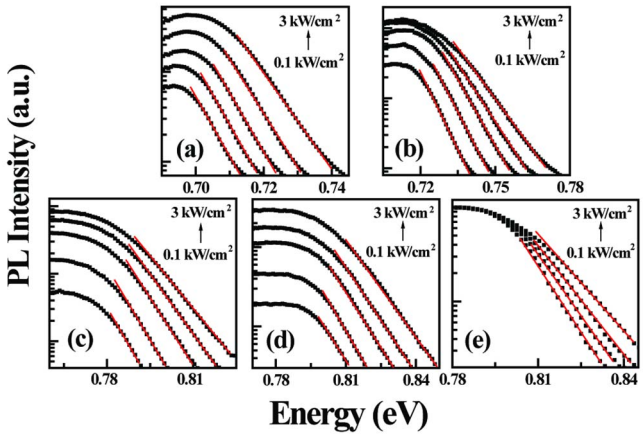

FIG. 1. (Color online) High-energy tails of PL of five InN samples with different free electron concentrations for different excitation densities: (a) 2.4×10^{18} cm^{-3}, (b) 3.3×10^{18} cm^{-3}, (c) 9.0×10^{18} cm^{-3}, (d) 1.3×10^{19} cm^{-3}, and (e) 1.6×10^{19} cm^{-3}. The solid lines represent the slopes of the high-energy tails. The excitation power density increases from 0.1 to 3 kW/cm^2.

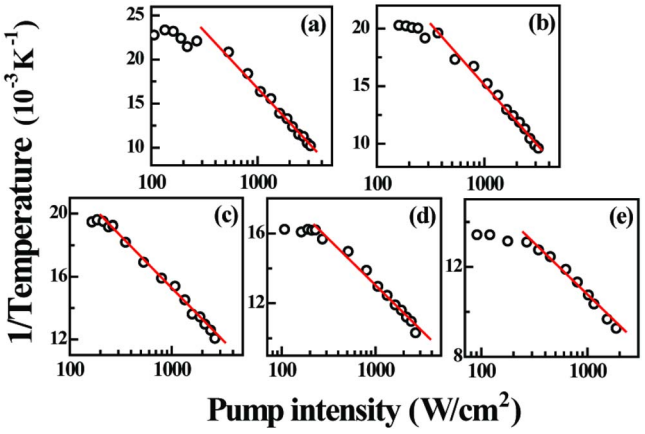

FIG. 2. (Color online) Inverse electron temperature vs pump intensity for five InN samples with different free electron concentrations. The solid lines correspond to slopes at which the activation energies can be extracted.

tion power for five InN samples with different free electron densities. In Fig. 2, the slopes of the inverse T_e are displayed as the solid lines for samples A to E, corresponding to values of 19, 24, 35, 52, and 63 meV, respectively. All these energies are below the LO phonon energy in InN (73 meV), indicating that the LO phonon is not the only phonon that governs the energy loss of hot electrons in InN. Restated, the energy relaxation of hot electrons in InN should include acoustic and optical phonons.

To determine the cooling mechanism that governs the relaxation of hot electrons, the rate of energy loss of acoustic and optical modes in InN was calculated. The rate of energy loss per electron due to the emission of acoustic phonons [including piezoelectric (PE) and deformation potential modes] is given by[14]

$$P_{e,\mathrm{ac}}(T_e) = \frac{3(m^*)^2 k_F}{\pi\rho\hbar^3}\left(A_c^2 + \frac{2}{5}\frac{C_{\mathrm{LA}}^2 + C_{\mathrm{TA}}^2}{k_F^2}\right)k_B(T_e - T_L), \tag{3}$$

where $k_F=(3\pi^2 n)^{1/3}$ is the Fermi wave vector, A_c is the conduction-band deformation potential, ρ is the mass density, and $C_{\mathrm{LA(TA)}}$ is the directionally averaged PE coupling constant for longitudinal (transverse) modes. For InN with the wurtzite crystal structure, C_{LA} and C_{TA} are given in terms of the three independent PE parameters, e_{15}, e_{31}, and e_{33}, by

$$C_{\mathrm{LA}} = \left\{\left(\frac{e}{\varepsilon}\right)^2\frac{1}{6}\left[\frac{4}{3}\left(e_{31} + \frac{3}{4}e_{33} + 2e_{15}\right)^2 + \frac{7}{4}e_{33}^2\right]\right\}^{1/2} \tag{4}$$

for longitudinal polarized phonons,[15] and

$$C_{\mathrm{TA}} = \left\{\left(\frac{e}{\varepsilon}\right)^2\frac{1}{8}\left[\left(e_{31} - e_{33} + \frac{1}{3}e_{15}\right)^2 + \frac{56}{9}e_{15}^2\right]\right\}^{1/2} \tag{5}$$

for transverse polarized phonons.[16] However, the energy loss per electron due to the emission of LO phonons is given by[14]

$$P_{e,\mathrm{LO}}(T_e) = \left(\frac{E_{\mathrm{LO}}}{\tau_{\mathrm{ph}}}\right)\left(\frac{e^{x_o - x_e} - 1}{e^{x_0} - 1}\right)\left[\frac{\sqrt{x_e/2}e^{x_e/2}K_0(x_e/2)}{\sqrt{\pi/2}}\right], \tag{6}$$

where τ_{ph} is the effective LO phonon lifetime, E_{LO} is the LO phonon energy, $x_0=E_{\mathrm{LO}}/k_B T_l$, $x_e=E_{\mathrm{LO}}/k_B T_e$, and K_0 is the modified Bessel function of order zero. Figure 3 plots the calculated average rate of energy loss in InN as a function of the electron temperature. In the calculations, the electron density was taken to be $n=2.4\times10^{18}$ cm^{-3} (the value for sample A). The open circles (solid triangles) are results calculated using Eq. (3) [Eq. (6)] and the solid line represents a combination of both equations. Figure 3 indicates that the energy relaxation of hot electrons proceeds mainly via acoustic phonon emission at electron temperatures <80 K. For electron temperature >80 K, the LO phonon emission dominates. This observation is in agreement with the experimental results in Fig. 2, revealing that the LO phonon is not the only phonon that contributes to the energy loss of the hot electrons.

To simulate the experimental rate of energy loss per electron, the total power loss rate P_{tot} is assumed to be a combination of $P_{e,\mathrm{LO}}$ and $P_{e,\mathrm{ac}}$,

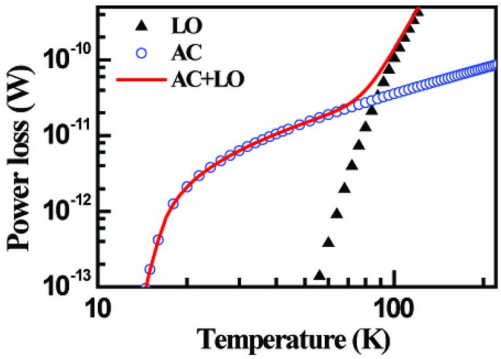

FIG. 3. (Color online) Calculated energy power loss in InN as function of the electron temperature. The acoustic (open circles) and LO (solid triangles) energy relaxation rates are calculated according to Eqs. (3) and (6), respectively. The line is a combination of both equations. The lattice temperature is $T_l=15$ K.

$$P_{\mathrm{tot}} = \chi P_{e,\mathrm{LO}} + (1-\chi)P_{e,\mathrm{ac}}, \tag{7}$$

where χ is the ratio of LO phonon emission to the acoustic phonon emission. Based on Eq. (7), the rate of energy loss rate, including that due to LO and acoustic phonon emission, is analyzed. However, the power balance equation is used to obtain the experimental power loss rate. In the steady state, the electron population increases with the excitation density, and enhanced electron-electron scattering increases the fraction of available energy that is shared with the electron gas. Thus, the electron temperature T_e can be determined by balancing the rate of generation of the energetic electrons with the rate of energy loss from the electrons to the lattice. For the photoexcitation the pump power per electron P_e given to the electron is given by[7]

$$P_e = \frac{I}{d}\frac{W}{\hbar\nu_0}\frac{1}{n}, \tag{8}$$

where I is the laser power absorbed per unit area, d is the absorption length at the laser energy, and W is the part of the photon excess energy obtained by an electron. Table I presents the values of the parameters used in Eq. (8). d was obtained by making optical absorption measurements (not shown). As displayed in Table I, d increases with n. Recently, Wu *et al.*[17] studied the effects of electron concentration on the optical absorption in InN. The electron concentration dependence of the optical absorption edge energy is explained by the free electron induced Burstein–Moss shift.[17] Based on their measurements, the absorption coefficient at a given excitation energy decreases as electron concentration increases. The increase in d with n can be thus understood by the Burstein–Moss effect since the absorption coefficient is inversely proportional to the absorption length. Figure 4 plots the dependence of power loss rate on the acoustic phonon emission, LO phonon emission, and a combination of both. The good agreement between the measured (the open circles) and the calculated (the solid lines) power loss rates indicates that the calculations should include both the acoustic and LO phonon emissions to explain the energy loss rate in InN. In the fits, χ increases with n, implying that the electron-LO-phonon interaction increases with n. As can be seen in Fig. 4, the dominant energy loss mechanism is the acoustic phonon

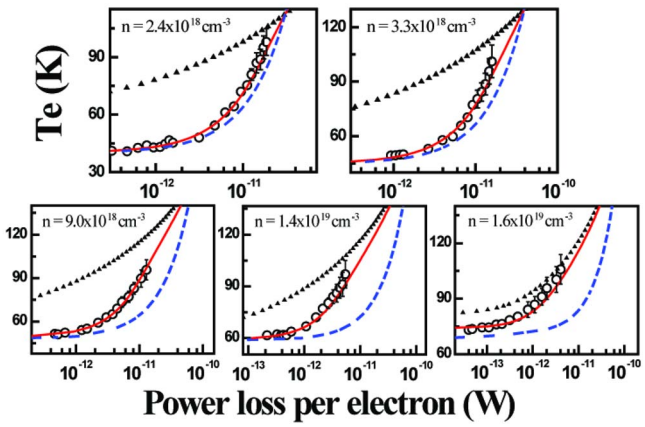

FIG. 4. (Color online) Measured electron temperature vs power loss rate for five InN samples with different free electron concentrations (open circles). Dependence of power loss rate on acoustic phonon emission (dashed line), LO phonon emission (solid triangles), and a combination (solid line) were calculated according to Eqs. (3) and (7), respectively.

emission for $n \leq 3.3 \times 10^{18}$ cm^{-3}. Crossover of the acoustic-LO phonon emission is observed as n increases, and the LO phonon emission becomes dominant for $n \geq 1.6 \times 10^{19}$ cm^{-3}. Notably, the LO phonon emission is always dominant in the high electron-temperature region (see Fig. 3).

Figure 5 plots the power loss rate as a function of n at a fixed electron temperature of 75 K (the data were extracted from Fig. 4). The energy loss rate decreases as n increases. Yoffa[18] explained the decrease in the energy loss rate at high electron density by the screening of the electron-polar optical phonon interaction. According to Yoffa's[18] calculations, the critical electron density n_c for the onset of screening in polar direct-gap semiconductors is

$$n_c = \frac{\varepsilon_s \hbar}{8\pi e^2 \sqrt{27}} \left[\frac{m^*}{k_B T_e} \right] \omega^3, \tag{9}$$

where ω is the phonon frequency and ε_s is the static dielectric constant. When the electron temperature is 75 K, a value of $n_c = 1.16 \times 10^{17}$ cm^{-3} is obtained. The screening of a high density of photogenerated electrons reduces the emission rate

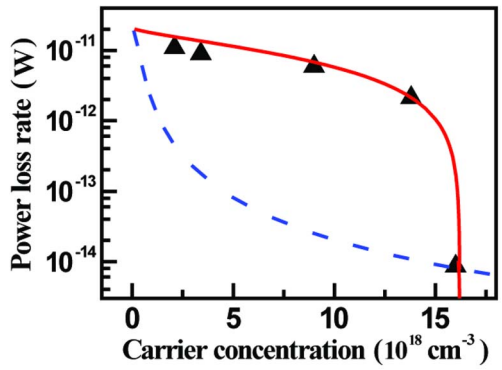

FIG. 5. (Color online) Measured power loss rate (solid triangles) as function of electron density at fixed electron temperature of 75 K. The dashed line represents dependence of the energy loss rate on electron density, determined by considering screening effect. The solid line represents the relationship between energy loss rate and electron density, according to $P_e \propto n^{2/3}$.

of phonons from hot electrons by a factor of $1+(n/n_c)^2$. The dashed lines in Fig. 5 represent the effect of screening on the energy loss rate, revealing that the screening of electrons cannot explain our results. However, the power loss rate P_e is proportional to $n^{2/3}$ for the PE interaction.[19] Based on this relation, the energy loss rate is simulated according to $P_e \propto n^{2/3}$, and the results are plotted as the solid line in Fig. 5. The calculated decrease in the power loss rate agrees closely with the experimental values. Thus, the reduction in the power loss rate at high electron density can be well explained by simply invoking the PE coupling to acoustic phonons.

IV. SUMMARY

The density-dependent energy relaxation of hot electrons is obtained from the excitation-dependent PL. The high-energy tails of PL can be characterized by effective electron temperatures, which increase with increasing excitation intensity. LO phonon emission alone cannot explain the relationship between the electron temperature and the electron energy loss rate. Instead, a model based on a combination of both the acoustic and LO phonon emissions can be used to explain the electron energy loss rate. Acoustic (LO) phonon emission is the dominant energy loss mechanism below (above) ~80 K. Reductions in the energy loss rate at high electron densities were observed in InN. The screening of the electron-LO phonon interaction does not affect the energy loss. However, the decrease in the energy loss rate is explained by invoking PE coupling to acoustic phonons.

ACKNOWLEDGMENTS

This project was supported in part by the National Science Council under Grant No. NSC97-2112-M-033-004-MY3 and the Institute of Nuclear Energy Research under Grant No. 962001INER0041.

[1] A. G. Bhuiyan, A. Hashimoto, and A. Yamamoto, J. Appl. Phys. **94**, 2779 (2003).
[2] K. S. A. Butcher and T. L. Tansley, Superlattices Microstruct. **38**, 1 (2005).
[3] B. Monemar, P. P. Paskov, and A. Kasic, Superlattices Microstruct. **38**, 38 (2005).
[4] T. Araya, N. Kato, and N. Otsuka, J. Appl. Phys. **98**, 043526 (2005).
[5] Y. Lou, M. Yin, S. O'Brien, and C. Burda, J. Electrochem. Soc. **152**, G427 (2005).
[6] S. S. Prabhu and A. S. Vengurlekar, J. Appl. Phys. **95**, 7803 (2004).
[7] J. Shah, Solid-State Electron. **21**, 43 (1978).
[8] F. Chen, A. N. Cartwright, H. Lu, and W. J. Schaff, Appl. Phys. Lett. **83**, 4984 (2003).
[9] D. Zanato, N. Balkan, B. K. Ridley, G. Hill, and W. J. Schaff, Semicond. Sci. Technol. **19**, 1024 (2004).
[10] M. D. Yang, Y. P. Chen, G. W. Shu, J. L. Shen, S. C. Hung, G. C. Chi, T. Y. Lin, Y. C. Lee, C. T. Chen, and C. H. Ko, Appl. Phys. A: Mater. Sci. Process. **90**, 123 (2008).
[11] K. T. Tsen, J. G. Kiang, D. K. Ferry, H. Lu, W. J. Schaff, H. W. Lin, and S. Gwo, Appl. Phys. Lett. **90**, 152107 (2007).
[12] G. W. Shu, P. F. Wu, Y. W. Liu, J. S. Wang, J. L. Shen, T. Y. Lin, P. J. Pong, G. C. Chi, H. J. Chang, Y. F. Chen, and Y. C. Lee, J. Phys.: Condens. Matter **18**, L543 (2006).
[13] M. Higashiwaki and T. Matsui, J. Cryst. Growth **269**, 162 (2004).
[14] K. Wang, J. Simon, N. Goel, and D. Jena, Appl. Phys. Lett. **88**, 022103 (2006).
[15] B. Jogai, J. Appl. Phys. **90**, 699 (2001).

[16]V. M. Naik, R. Naik, D. B. Haddad, J. S. Thakur, G. W. Auner, H. Lu, and W. J. Schaff, Appl. Phys. Lett. **86**, 201913 (2005).
[17]J. Wu, W. Walukiewicz, S. X. Li, R. Armitage, J. C. Ho, E. R. Weber, E. E. Haller, H. Lu, W. J. Schaff, A. Barcz, and R. Jakiela, Appl. Phys. Lett. **84**, 2805 (2004).
[18]E. J. Yoffa, Phys. Rev. B **23**, 1909 (1981).
[19]N. M. Stanton, A. J. Kent, A. V. Akimov, P. Hawker, T. S. Cheng, and C. T. Foxon, J. Appl. Phys. **89**, 973 (2001).